Title

Adaptive motivational signalling from the anterior cingulate cortex and ventral tegmental area

Abbreviated title

Adaptive motivation signals in the ACC and VTA

Authors and Affiliations

Thomas W. Elston[1,2]* & David K. Bilkey[1,2]

(1) Brain Health Research Centre, University of Otago
(2) Department of Psychology, University of Otago, Dunedin, New Zealand

Corresponding author contact

telston@postgrad.otago.ac.nz

Number of materials and word counts

Figures: 8

Tables: 5

Abstract: 148 words

Introduction: 616 words

Discussion: 1228 words

Abstract

Information gained during goal pursuit motivates adaptive behaviour. The anterior cingulate cortex (ACC) supports adaptive behaviour, but how ACC signals are translated into motivational signals remains unclear. Rats implanted in the ACC and ventral tegmental area (VTA), a dopaminergic brain area implicated in motivation, were trained to run laps around a rectangular track for a fixed reward, where each lap varied in physical effort. Partial directed coherence analysis of local field potentials indicated strong ACC-driven increases in VTA theta (4-12 Hz) power as well as elevated running speed as rats entered the effort-containing region of the maze on trials when the effort was absent. No increases were detected on effortful trials. These data suggest that ACC provides a top-down modulating signal which can influence the motivation with which to pursue a reward. We discuss several interpretations and conclude that our findings are, perhaps, a neural correlate of relief.

Introduction

Adaptation to changing circumstances is a common, critical consideration in nature (Darwin, 1865); however, the neural mechanisms enabling adaptive goal-directed behaviour have yet to be fully elucidated. The anterior cingulate cortex (ACC), a subregion of the anterior medial prefrontal cortex (AC), signals predictions of future reward and errors in such predictions and received reward (Bryden, Johnson, Tobias, Kashtelyan, & Roesch, 2011; Kennerly, Behrens, & Wallis, 2011). These signals are thought to provide an attention for learning signal, facilitating the integration of new information into existing internal representations which can motivate and adapt future behaviour (Bryden et al., 2011; Cavanagh, Frank, Klein, & Allen, 2010). However, it remains unclear how ACC signals are translated into an adaptive, motivational signals.

The ACC and the anterior portions of the medial prefrontal cortex, broadly, exert direct top-down control over the ventral tegmental area (VTA) via monosynaptic glutamatergic afferents (Beier et al., 2015; Faget et al., 2016; Ferenczi et al., 2016; Taber, Das, & Fibiger, 1995) and becomes dysfunctional in pathological goal-seeking states, such as nicotine addiction (Wu et al., 2013) and severe apathy (Njomboro, Deb, & Humphreys, 2012). Rodent single unit studies report large and transient spikes of activity in both ACC and VTA, respectively, when an outcome is different than predicted (Bryden et al., 2011; Eshel, Tian, Bukwich, & Uchida, 2016). Strikingly, in both ACC and VTA, the magnitude of the activity increase correlates with the magnitude of the prediction error (Bryden et al., 2011; Eshel et al., 2015; Kennerly et al., 2011). The VTA is a major source of dopamine to the basal ganglia and is hypothesized to convey a motivational signal indicating progress towards and value of a future goal (Hamid et al., 2016; Howe, Tierney, Sandberg, Phillips, & Graybiel, 2013; Morales & Margolis, 2017; Salamone & Correa, 2012). Thus, ACC top-down control over dopaminergic subcortical regions, such as the VTA, is a plausible mechanism by which ACC signals are translated into motivational signals.

Although no prior study has jointly examined the relationship between the ACC and VTA, prior investigations of anterior cortical (AC) and VTA communication suggest that these structures communicate via oscillations in the theta band (4-12 Hz). For example, firing in VTA dopamine neurons is modulated by the phase of AC theta oscillations and AC-VTA synchronization in the theta band is strongly correlated with working memory performance (Fujisawa & Buzsaki, 2011; Gao, Yang, Jin, Bunney, Shi, 2007). This notion is consistent with human EEG and monkey single unit experiments which found transient increases in human frontal theta power and monkey ACC unit firing when outcomes violated expectations which then led to adaptive behaviour (Cavanagh et al., 2010; B. Y.

Hayden, Heilbronner, Pearson, & Platt, 2011). However, to date, the precise relationship between the ACC and VTA and how these signals might shape future behaviour remains unknown.

To address this question directly, we monitored ACC and VTA local field potentials (LFPs) of rats trained to run laps around a rectangular track for a fixed reward, where each lap randomly varied in physical effort. The effortful condition required rats to climb over a 30cm barrier while no barrier was present in the non-effortful condition. In addition to task-dependent changes in theta (4-12 Hz) power and coherence, we also assessed the directionality of communication between ACC and VTA via partial directed coherence (PDC), a multivariate autoregressive modelling approach which provides a frequency-resolved estimate of Granger causality (Baccalá & Sameshima, 2001; Boykin, Khargonekar, Carney, Ogle, & Talathi, 2012). We predicted that in the absence of additional physical effort, when there has been in the past, theta power and coherence in the VTA and ACC and running speed in the barrier-containing region would increase in an ACC-driven, top-down manner.

Methods

Subjects

Seven male Sprague Dawley rats (Hercus-Taieri Resource Unit) weighing 450-550 g were used in the study. Rats were single housed in translucent plastic cages containing pine chips and maintained on a 12 h light/dark cycle. All training and experimentation occurred during the light phase. After 2 weeks of daily handling and weighing, animals were food deprived of standard rat chow (Specialty Feeds) to no less than 85% of their free-feeding weight to promote interest in food reward during test phases. Water was available *ad libitum* in the home cage.

Preoperative training

During the initial week of training, rats were individually habituated for 15 min/d to the experimental apparatus, a rectangular runway with a reward area (Figure 1) which contained touchscreens, photobeams, and a retractable 30cm barrier which was mounted on a servo motor; the apparatus was controlled by a network of four Arduino (Arduino LLC, Somerville, MA, USA) microcontrollers. Cereal pellets (Coco Pop cereal; Kellogg's) were scattered throughout the maze to encourage exploration. In the second week of training, cereal pellets were only available at the reward site and rats were trained to run the maze in a unidirectional manner, starting at the bottom of the midstem (i.e. the startbox) and

128 received a fixed reward (3 cocopops) in a distinct reward zone. Rats were prevented from
129 reversing course in the maze by photobeam-controlled doors. The rats were not paused
130 between trials and set their own pace, running in a continuous, uninterrupted manner.

131 Once the rats were running unidirectionally around the apparatus, they were trained
132 to press a wall-mounted touchscreen to release an adjacent starting gate and thereby initiate
133 a new trial. This typically took two 15 minute training sessions or less. A two-second delay
134 was then introduced between the initial press and the lowering of the start gate. Screen-
135 press training was considered complete when rats ran >30 trials/session (2/min) across 3
136 consecutive training sessions. This typically took one week of training.

137 The final stage of training involved the introduction of a 30cm barrier into the
138 apparatus which rats had to overcome on their route to the reward zone. The barrier was
139 randomly inserted into the maze by a servo motor. Rats were cued as to whether the
140 upcoming trial was an effortful, barrier trial or a non-effortful, flat trial by images delivered
141 on the touch screen. The screen displayed three flashing green horizontal bars on a black
142 background across the screen to indicate a barrier trial and a single non-flashing white bar
143 on a magenta background to indicate a flat trial. To provide auditory camouflage for barrier
144 insertion, the barrier was placed into the maze at the same instant the start gate was
145 opened. Once rats were running >30 trials/session, sessions were extended such that each
146 session required rats to run 120 laps composed of 60 trials without the barrier present (flat
147 trials) and 60 barrier trials presented in pseudo-random order. Rats were considered fully
148 trained when they were running 120 trials within 60 minutes (2/min).

149 **Surgery**

150 Once animals were considered trained, five rats were anaesthetized under isoflurane
151 and stereotaxically implanted in the ACC (AP: 2.7mm, ML: 0.4mm, DV: -1.8mm from dura)
152 with 25 µm Formvar-coated nichrome wires (California Fine Wire) mounted on a 3D-
153 printed adjustable microdrive assembly and the VTA (AP: -5.3mm, ML: 1.0mm, DV: -
154 8.2mm from dura) with a one non-moveable 127-µm-diameter, nickel-chromium coated
155 wire. Two rats were also implanted at the same ACC coordinate with the microdrive
156 assembly but with a second electrode (a fixed 127-µm-diameter, nickel-chromium coated
157 wire) located in the dorsal CA1 subregion of the hippocampus (AP: -3.6mm, ML: 2.0mm,
158 DV: -2.8mm from dura). The electrodes were grounded by soldering a wire to a jewellers
159 screw implanted in the cerebellum. The assembly was fasted to the skull with jeweller's
160 screws and acrylic dental cement. Following the surgery, animals were allowed 10 days to
161 recover during which they had *ad libitum* food and water. After 10 days, rats' food was

reduced to maintain the animal at ~85% of their free-feeding weight to optimize behaviour during the experiment.

Postoperative training and protocol

After 10 days of recovery, rats were reintroduced to the maze with the head plugs connected to a tethered head stage that housed three light emitting diodes (LEDs) for tracking. Training resumed from the final preoperative stage; all 7 rats quickly recalled the task with no signs of postoperative motor impairment. Once each rat demonstrated three consecutive sessions of 120 trials in less than one hour, data acquisition began.

The data acquisition protocol consisted of a three stage, 'ABA' design (Figure 1): seven days with protocol B1, during which the barrier was present in 50% of trials, three days extinction, during which touchscreen cues remained and the barrier was either 0% or 100% present, regardless of the cue, and three days of B2, in which the barrier was present in 50% of trials. Four rats experienced the 100% barrier-present condition during the second stage and three rats experienced the 0% barrier phase. All seven rats experienced B1 and B2. It should be noted that the rats probably did not attend to the cues as there was no behavioural relevance to them and we found no behavioural or electrophysiological evidence that the cues themselves elicited any specific response.

Electrophysiological recordings and data acquisition

Local field potentials were recorded using the dacqUSB multichannel recording system (Axona Ltd.). Local field potentials were low-pass filtered at 500 Hz, and sampled at 4800 Hz. The animals' position was monitored by a ceiling-mounted video camera connected to a tracking system that monitored the LEDs mounted on the head stage. Tracking data was sampled at 50 Hz and made available to the dacqUSB system. Key events (e.g. trial initiation, the type of trial initiated, when rats got to the barrier region, and when rats reached the reward) were timestamped by inputs from a custom-built neural network of Arduino microcontrollers connected to a digital input-output port on the dacqUSB system.

Data analysis

All analyses were conducted using MATLAB R2015b (The Mathworks, Boston, MA, USA). Power spectral density (PSD) data for the whole dataset were initially determined using using Welch's estimate method, *pwelch* in MATLAB. Time resolved LFP power and coherence was then calculated via multi-taper spectrograms and coherograms which used 3 tapers, a reading window of one second, and 85% overlap amongst windows. Data was

linearized by dividing the maze path into 9 bins of 3-5cm in length and the position timestamps of rats entering and exiting a given region on a given lap on a given trial type were used to collect relevant pieces of the spectrogram and coheragram which were then averaged for each maze region on each lap, separately. A similar approach was used to collect instantaneous speed data from each maze region for each lap on a given trial type. Task-related causal relationships between ACC-VTA and ACC-dCA1, linearly detrended LFPs were assessed with a partial directed coherence (PDC) algorithm, a frequency-resolved measure of Granger causality which uses multivariate autoregressive modelling to exploit the predictability of information in one brain area by past activity in another (Baccalá & Sameshima, 2001; Boykin, Khargonekar, Carney, Ogle, & Talathi, 2012).

Upon completion of the study, rats were deeply anaesthetized with isoflurane and recording sites were marked with direct current (2mA for 2 s) before transcardial perfusion. Electrode tracks and microlesions marking the electrode position were identified in 32µm thick sections of formalin-fixed tissue stained for Nissl substance (see Figure 2B).

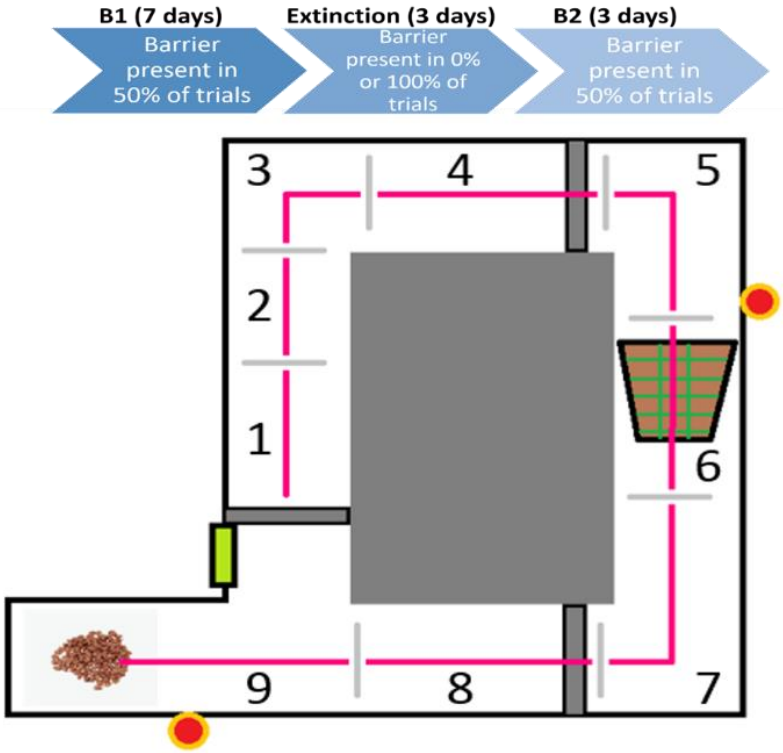

Figure 1. Schematic of maze and protocol. Rats initiated laps by pressing a wall-mounted touchscreen. After a 2-second delay, the startbox door opened and rats ran through regions 1-9. The experiment consisted of 3 phases: B1 (50% barrier), extinction (either 0% barrier or 100% barrier), and B2 (50% barrier).

Results

A

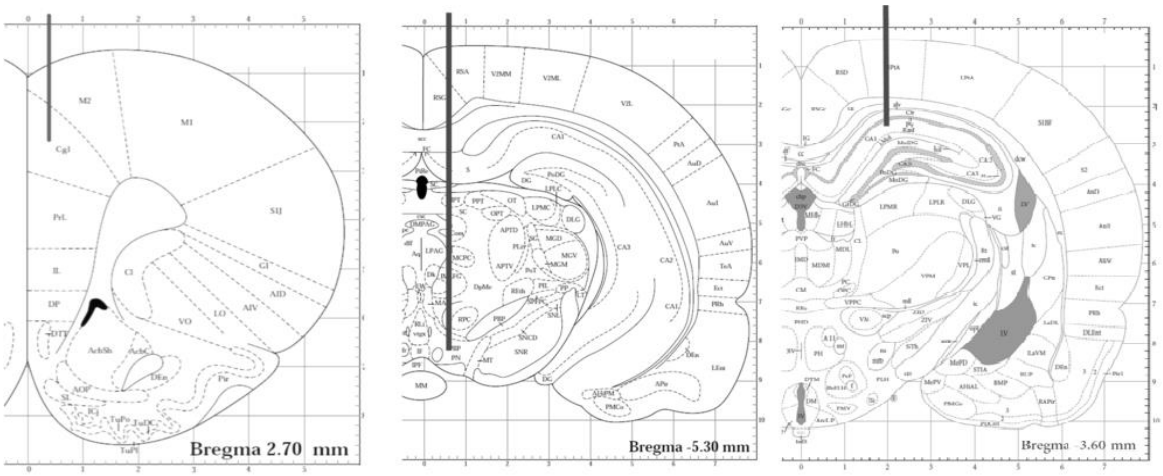

B

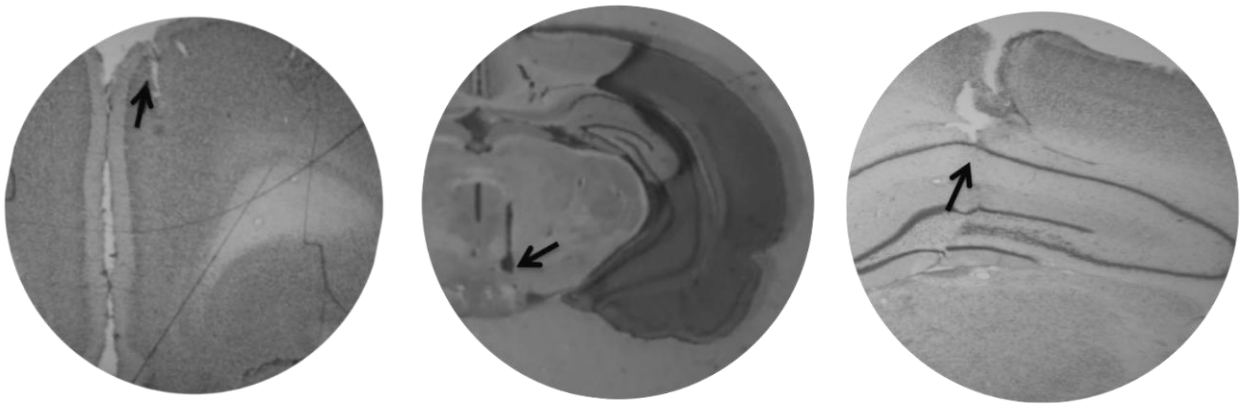

C

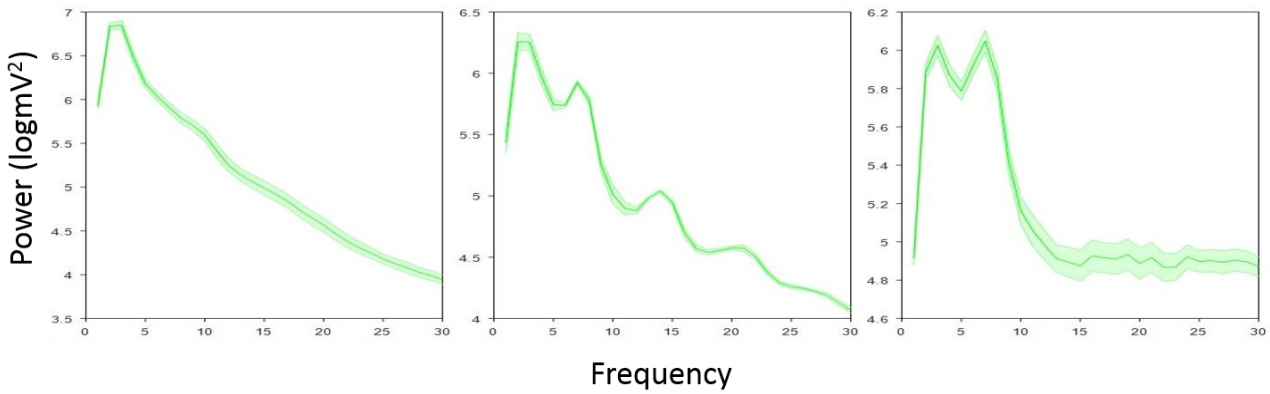

Figure 2. **A.** Plates from Paxinos & Watson (1997) indicating electrode placement in ACC (AP: 2.7mm, ML: 0.4mm, DV: -1.8mm from dura), VTA (AP: -5.3mm, ML: 1.0mm, DV: -8.2mm from dura), and dCA1 (AP: -3.6mm, ML: 2.0mm, DV: -2.8mm from dura). **B**. Histology indicating electrode placement in ACC, VTA, and dCA1. **C.** Power spectrum densities (PSDs) determined via Welch's estimate method for ACC, VTA, and dCA1, in that order. The solid lines indicate the mean and the shaded areas are the standard errors.

214 **Task-modulated theta oscillations in ACC and VTA**

215 LFP patterns in ACC, VTA, and dCA1 were characteristically different with PSD
216 functions from the ACC having a peak at low theta frequencies (3-5 Hz), while both VTA and
217 dCA1 exhibited prominent peaks in both the high theta band (7-9 Hz) and low theta band
218 (3-5 Hz; Figure 2C). When the LFP data were examined on a region by region basis it was
219 apparent that during phase B1, when the barrier was present 50% of the time, there was a
220 marked difference in theta power, in both the VTA and ACC, and in the coherence between
221 them, when the barrier-absent and barrier-present trials were compared (Figure 3). In
222 barrier-absent trials there was a significant increase in low theta power and coherence that
223 began once the animal reached the second turn (region 5) of the maze. Power increased
224 until the barrier region and then although decreasing slightly, was sustained above the level
225 measured in the starting stem until, and including, the reward zone (region 9). In barrier-
226 present trials, however, theta power and coherence did not increase at region 5 ($p < .005$ for
227 regions 5-8, respectively, t-tests). Rather, levels remained supressed from the initial turn
228 through until the reward region, at which point ACC and VTA theta power and coherence
229 increased suddenly to become equivalent to that observed in barrier absent trials. This was
230 a large effect (Hedge's $g > 1$ for regions 5-8, respectively) and was observed across all
231 animals, independently producing significant within-subject effects for every animal
232 (regions 5-8, $p < .0005$, t-tests; see Figure 4 for all examples). No significant difference in
233 ACC and VTA theta power or coherence was detected in the reward zone for any animal
234 (region 9, all $p > .05$, t-tests).

235 In phase 2, the barrier was either not present for all trials ($n = 4$ animals) or was
236 present for all trials ($n=3$ animals) irrespective of the cue on the touchscreen, which
237 continued to randomly signal the two types of trials on a 50% basis. For animals where the
238 barrier was absent, an abrupt increase in ACC and VTA theta power, similar to that which
239 occurred in no-barrier trials in phase B1, was detected from regions 5 through 8 in all
240 animals regardless of the trial type cued by the touch screen (Figure 5). For animals where
241 the barrier was present on all trials, theta power remained low across these regions,
242 replicating the effect of barrier-present trials in B1 (Figure 3). An analysis to determine
243 whether the, now irrelevant and probably ignored, cue signal altered responses during
244 phase 2 revealed no significant differences in ACC and VTA responses in regions 5 to 8
245 following the two cue types (all $p > .05$, t-tests).

246 In the third phase, B2, the barrier was again present on 50% of trials. In a result that
247 replicated condition B1, an abrupt increase in running speed, ACC and VTA theta power,
248 and coherence was detected in regions 5-8 in all animals when the barrier was absent

(Figure 3; all p < .005, t-tests). On barrier trials, power and coherence remained suppressed until the reward region. Again, ACC and VTA theta power and coherence in the reward zone (region 9) did not depend on the trial type (p > .05, t-test). Analysis of responses across the multiple trials of each condition revealed that the significant modulation of ACC and VTA theta power and coherence by the presence or absence of the 30cm barrier in the barrier-containing region of the maze (region 6) was consistent across days and trial conditions (Figure 5).

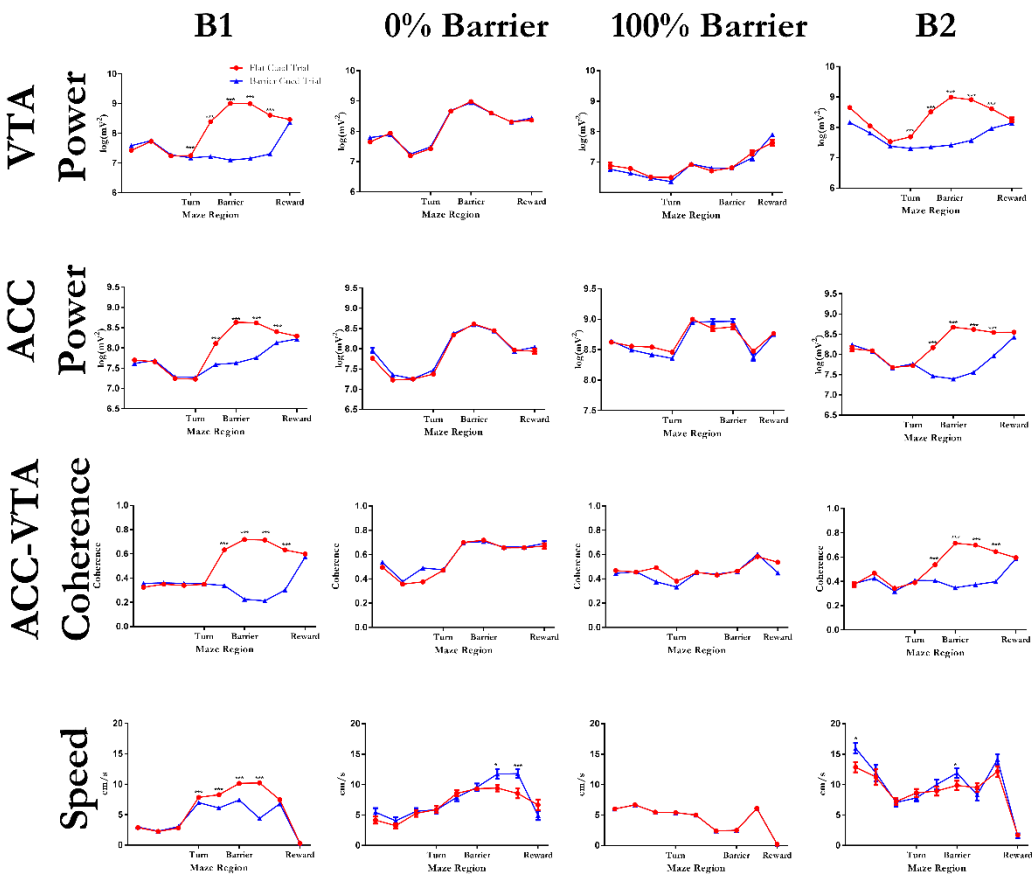

Figure 3. Enhanced theta (4-12Hz) power and coherence corresponds with the absence of the barrier. ACC and VTA time-resolved theta power, theta coherence, and running speed as a function of position for rat A (B1, 0%, and B2; mean ± SEM; n = 350 trials for B1, n = 150 trials for 0% barrier, and n = 150 trials for B2) and rat T (100% barrier; mean ± SEM; 150 trials for 100% barrier). The average power and coherence between 4 and 12 Hz for each region on each lap was used. *p < .05, **p < .005, ***p < .0005

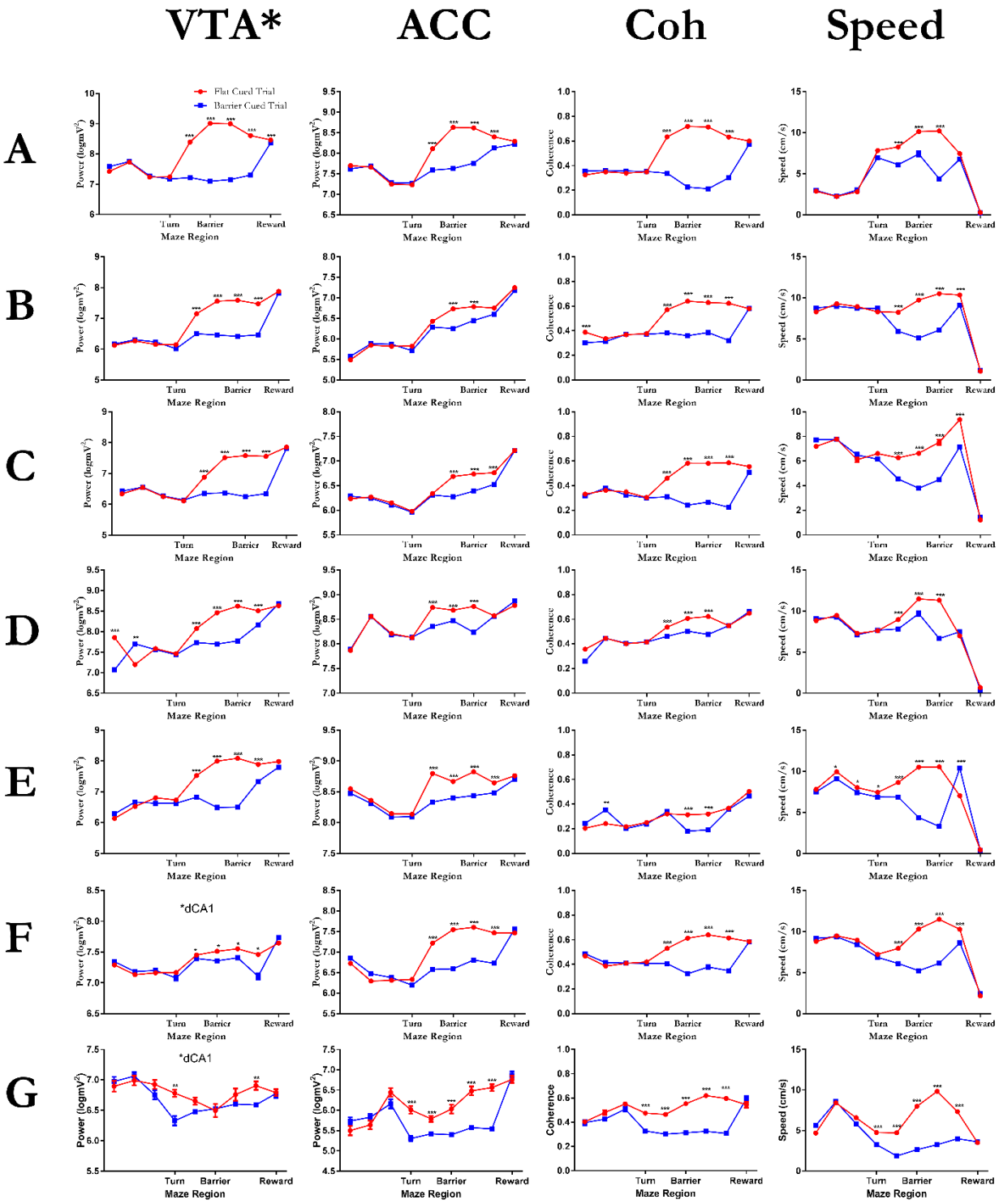

Figure 4. Enhanced theta (4-12Hz) power and coherence corresponds with the absence of the barrier in all rats. A. Data from all rats in phase B1. Rat name is listed on the left and brain region is listed along the top. *Data for rats F and G in the VTA column are dCA1 data.

261

262

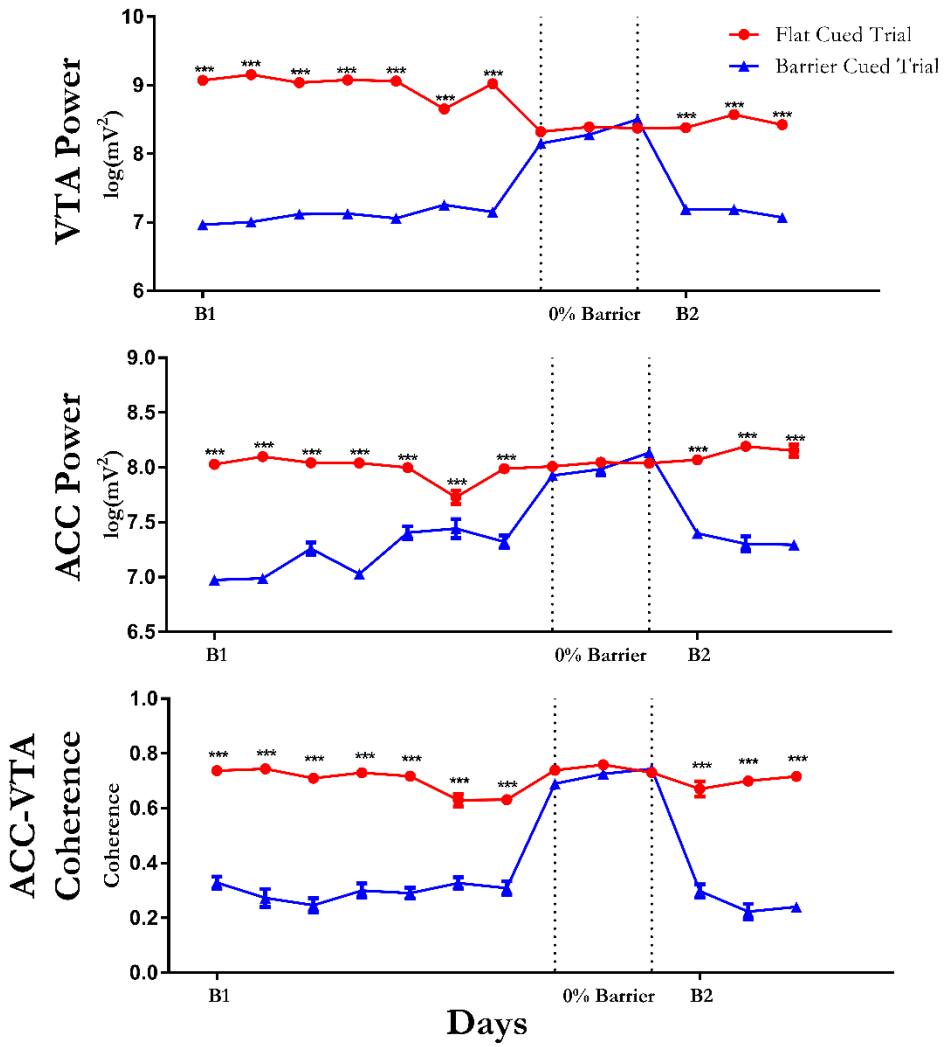

Figure 5. ACC and VTA theta and coherence responses to the presence or absence of the 30cm barrier in the barrier-containing region (region 6) of the maze were consistent across days and conditions. Data shown from rat A. VTA and ACC theta power and coherence were greater on trials when the barrier was present than when the barrier was absent across all days of B1 and B2 ($p < .005$, t-tests). *$p < .05$, **$p < .005$, ***$p < .0005$

Task-modulated theta oscillations in ACC and dCA1

To determine whether we were detecting a brain-wide phenomenon or activity that might be confined to specific regions, including VTA and ACC, we implanted 2 rats in both dCA1 and ACC and ran these animals through the procedure. As we had shown previously, in phase B1, we detected abrupt and sustained increases in ACC theta power from region 5 to 8 on no-barrier trials compared to barrier trials ($p < .005$, t-tests) in both animals (see Figures 4 and 6). In the second phase, when the barrier was absent on all trials, a similar abrupt increase in ACC theta power was detected regardless of the, likely ignored, cue ($p > .05$, t-tests). In phase B2, a significant difference in ACC theta power was detected in

regions 5 to 8 when barrier and no-barrier trials were compared (all $p < .005$, t-tests) as we had observed previously. By comparison, recordings from dCA1 showed that there was a much smaller increase in theta power in regions 5-8 in B1 no-barrier trials. The difference between barrier and no-barrier trials was statistically significant ($p < .05$, t-test; Figure 4) in one animal but not the other ($p > .05$, t-test) in phase B1. In phase B2, however, no significant barrier-related changes were detected in dCA1 theta power in either animal ($p > .05$, t-tests, Figure 6). Despite the minimal effects seen in dCA1 theta power, ACC-dCA1 theta coherence was significantly modulated by the presence or absence of the 30cm barrier. In phases B1 and B2 dCA1-ACC theta coherence abruptly increased in region 5 and remained elevated through region 8 in no barrier trials compared to barrier trials ($p < .005$, t-tests). In phase 2, when the barrier was never present, a similar abrupt and sustained elevation in theta coherence, beginning in region 5, was detected regardless of the cued condition ($p > .05$, t-tests).

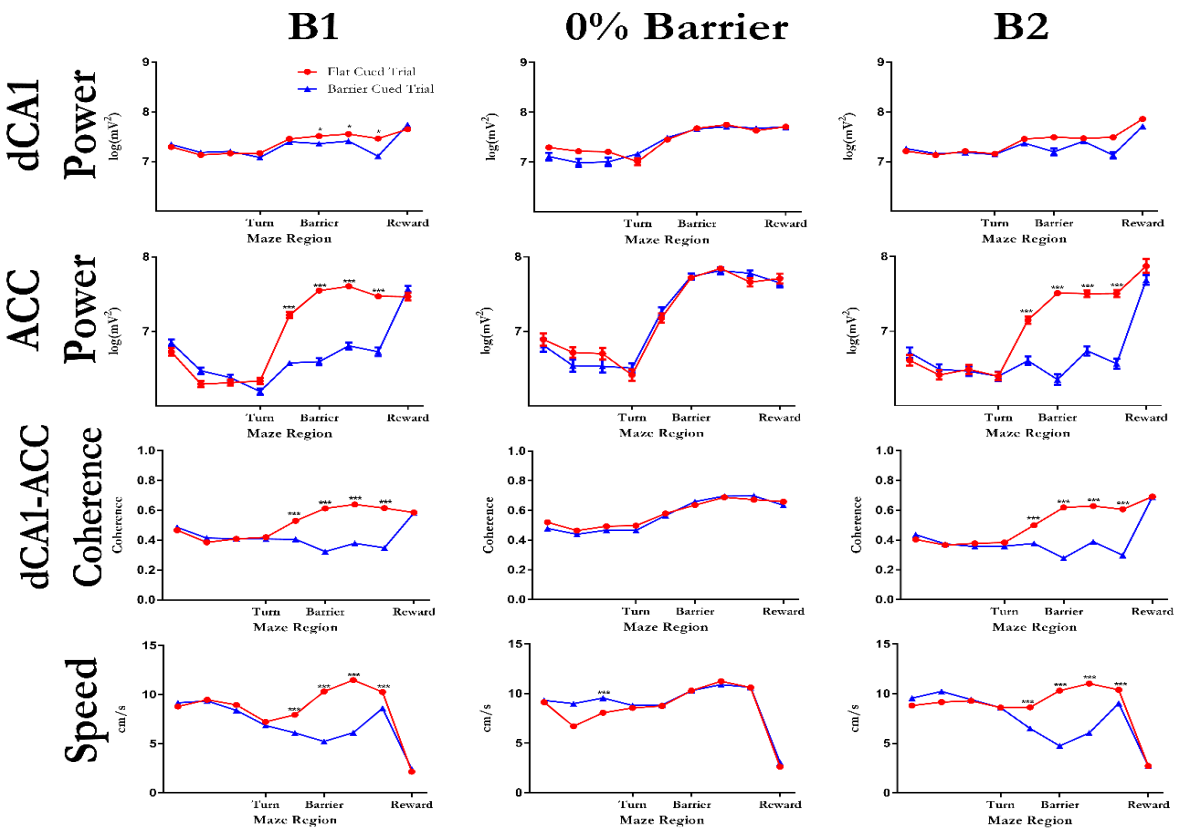

Figure 6. ACC but not dCA1 theta power was significantly modulated by the presence or absence of a 30cm barrier. Data are from Rat F. (mean ± SEM; n = 350 trials for B1, n = 150 trials for 0% barrier, and n = 150 trials for B2) *$p < .05$, **$p < .005$, ***$p < .0005$

Relationship to running speed

We were concerned that our results may have simply been an artefact of changes in running speed; indeed, at first glance, the patterns of power and coherence seemed to parallel changes in speed (Figure 3). However, upon closer inspection, it's clear that running speed and LFP power and coherence are not always changing together. For instance, an increase in running speed occurred in region 4 before the increase in power and coherence was observed (region 5). Furthermore, while running speed is near zero in the reward region, LFP power and coherence is elevated. To formally assess the relationship between running speed and LFP dynamics, we conducted correlations (Pearson's R) between the instantaneous running speed and instantaneous theta power (4-12Hz) in ACC, VTA, and dCA1, respectively, across all sessions, separately for each rat, considering only instances when rats were moving (e.g. speed > 1). All correlation coefficients were near zero and none were significant (all $r < 10^{-2}$, all $p > .05$; see Figure 7A-C and Table 1), suggesting that speed and power were independently driven by the effort condition. To directly examine the relationship between running speed, LFP dynamics, and the effort condition in the barrier region, we conducted analyses of covariance (ANCOVA) with instantaneous ACC, VTA, or dCA1 theta power, respectively, in the barrier region as the dependent variable, the corresponding instantaneous running speed as a covariate, and the presence or absence of the barrier as the independent variable for all sessions of phase B1 for each animal, separately. Resultant ANCOVAs revealed a significant relationship between VTA, ACC, and dCA1 theta power in the barrier region (see Table 2); however, after statistically controlling for running speed as a covariate, the presence or absence of the barrier remained a highly significant factor in the ACC and VTA, but not dCA1, in all rats (all $p < .0005$; see Table 3). These results indicate that running speed and VTA and ACC theta power are independently modulated by the effort condition, whereas dCA1 theta power was dependent on running speed.

Table 1.
Correlations Between Running Speed and LFP Theta (4-12 Hz) Power by Brain Region and Rat

Rat	VTA and Running Speed	ACC and Running Speed	dCA1 and Running Speed
A	$r(16693) = -1.76\times10^{-5}$, $p > .05$	$r(16693) = -1.90\times10^{-3}$, $p > .05$	
B	$r(96303) = -1.70\times10^{-4}$, $p > .05$	$r(96303) = -6.49\times10^{-4}$, $p > .05$	
C	$r(106428) = -1.53 \times 10^{-4}$, $p > .05$	$r(106428) = -6.09 \times 10^{-4}$, $p > .05$	
D	$r(145577) = 2.40 \times 10^{-3}$, $p > .05$	$r(145577) = -1.80 \times 10^{-4}$, $p > .05$	
E	$r(159581) = 4.00\times10^{-3}$, $p > .05$	$r(159581) = 6.4\times10^{-3}$, $p > .05$	
F		$r(78535) = 3.55\times10^{-4}$, $p > .05$	$r(78535) = 2.90\times10^{-4}$, $p > .05$
G		$r(123664) = 5.10\times10^{-3}$, $p > .05$	$r(123664) = 5.8\times10^{-3}$, $p > .05$

Table 1. Running speed – LFP theta (4-12 Hz) power correlation statistics for all rats.

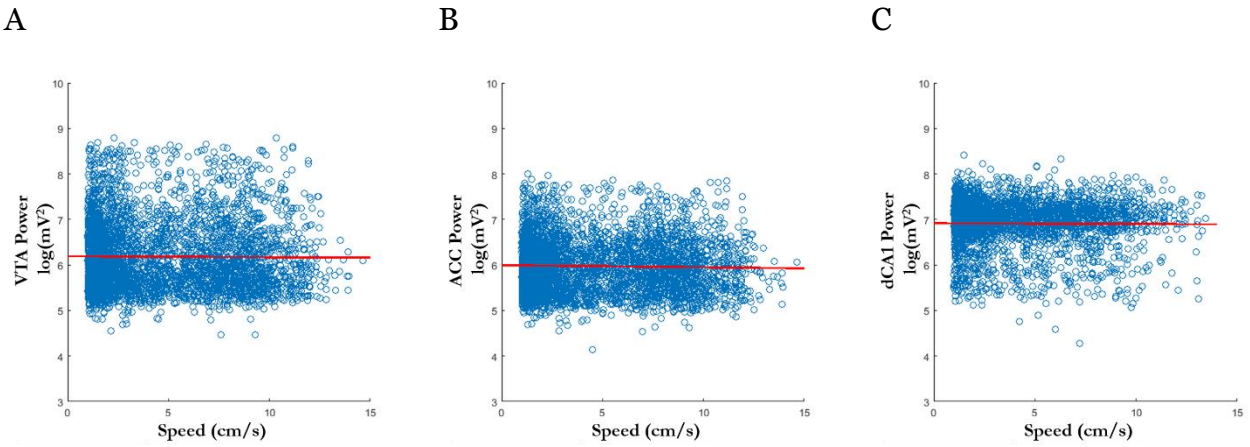

Figure 7. Relationships between running instantaneous speed and instantaneous LFP theta power while rats moved > 1 cm/s. **A.** Data from rat A showing the correlations between running speed and VTA theta power. **B.** Data from rat A showing the correlations between running speed and ACC theta power. **C.** Data from rat F showing the correlations between running speed and dCA1 theta power, respectively.

Table 2.
B1 ANCOVA Results for Theta (4-12 Hz) Power and Speed Relationship by Brain Region and Rat

Rat	VTA Theta Power	ACC Theta Power	dCA1 Theta Power
A	$F_{1,116828}= 6.95x10^{3}$, $p<1.00x10^{-200}$	$F_{1,82363}= 3.52x10^{3}$, $p<1.00x10^{-200}$	
B	$F_{1,35669}= 4.59x10^{3}$, $p<1.00x10^{-200}$	$F_{1,35669}= 2.30x10^{3}$, $p<1.00x10^{-200}$	
C	$F_{1,52251}= 2.65x10^{3}$, $p<1.00x10^{-200}$	$F_{1,52251}= 6.83x10^{2}$, $p=1.25x10^{-149}$	
D	$F_{1,40881}= 3.81x10^{3}$, $p<1.00x10^{-200}$	$F_{1,40881}= 7.51x10^{3}$, $p<1.00x10^{-200}$	
E	$F_{1,73924}= 9.53x10^{3}$, $p<1.00x10^{-200}$	$F_{1,73924}= 2.91x10^{3}$, $p<1.00x10^{-200}$	
F		$F_{1,45583}= 2.01x10^{3}$, $p<1.00x10^{-200}$	$F_{1,82363}= 179.25$, $p=8.41x10^{-41}$
G		$F_{1,82363}= 104.43$, $p<1.00x10^{-200}$	$F_{1,82363}= 4.96x10^{3}$, $p<1.00x10^{-200}$

Table 2. ANCOVA results indicating significant covariance between theta power and running speed.

Table 3.
B1 ANCOVA Results for Barrier Presence After Controlling for Run Speed by Brain Region and Rat

Rat	VTA Theta Power	ACC Theta Power	dCA1 Theta Power
A	$F_{1,116828}= 9.17$, $p=2.50x10^{-3}$	$F_{1,82363}= 4.38$, $p=5.00x10^{-3}$	
B	$F_{1,35669}= 1.77x10^{3}$, $p<1.00x10^{-200}$	$F_{1,35669}= 493.64$, $p=1.26x10^{-108}$	
C	$F_{1,52251}= 2.52x10^{3}$, $p<1.00x10^{-200}$	$F_{1,52251}= 5.79x10^{3}$, $p<1.00x10^{-200}$	
D	$F_{1,40881}= 2.19x10^{3}$, $p<1.00x10^{-200}$	$F_{1,40881}= 507.99$, $p=8.38x10^{-112}$	
E	$F_{1,73924}= 2.05x10^{3}$, $p<1.00x10^{-200}$	$F_{1,73924}= 169.73$, $p=9.35x10^{-39}$	
F		$F_{1,45583}= 661.15$, $p=9.11x10^{-145}$	$F_{1,82363}= 3.43$, $p>.05$
G		$F_{1,82363}= 7.23$, $p=3.26x10^{-4}$	$F_{1,82363}= 1.37$, $p>.05$

Table 3. ANCOVA results for factor barrier presence as a significant predictor of theta power in ACC and VTA after adjusting for running speed as a covariate.

ACC top-down influence over dCA1 and VTA is modulated by barrier presence

We then used a partial directed coherence (Baccalá & Sameshima, 2001) procedure following Boykin, Khargonekar, Carney, Ogle, & Talathi (2012)'s method to determine if there was evidence of signal directionality in linearly detrended LFPs recorded simultaneously from ACC and VTA and ACC and dCA1 as the animal passed through the barrier-containing region (region 6) of the maze. The mean partial directed coherence (PDC) was calculated in a trial-by-trial manner in each condition for data in the theta range (4-12 Hz). To verify the integrity of our PDC modelling, we scrambled the recorded signals from both ACC and VTA and conducted the trial-by-trial PDC analysis again. In every case the mean of the permutated PDC distribution was significantly weaker than the non-permuted data (all PDC < $3x10^{-5}$, all p < $3.76x10^{-36}$), losing evidence for directionality. An ANOVA examining the resultant PDC between ACC and VTA in B1 revealed significant main effects of directionality ($F_{1,194}$ = 719.45, p = 2.01 x 10^{-124}) and barrier condition ($F_{1,1194}$ = 121.57, p = 5.46 x 10^{-27}) as well as a significant directionality x barrier interaction effect on ACC-VTA theta PDC responses ($F_{1,1194}$ = 151.02, p = 9.03 x 10^{-33}; see Figure 8A; see Table 4 for data from all rats). An ANOVA considering B2 returned nearly identical results (see Table 5). This interaction is a result of ACC → VTA PDC being higher when the barrier was absent and decreasing in barrier trials while VTA→ACC PDC remained low and unchanging across conditions. Similarly, an ANOVA examining PDC between ACC and dCA1 across all trials and conditions revealed significant main effects of directionality ($F_{1,1797}$ = 207.32, p = 5.3 x 10^{-44}) and barrier presence ($F_{1,1797}$ = 233.09, p = 1.43 x 10^{-49}) as well as a significant directionality x barrier interaction effect on ACC-dCA1 theta PDC responses ($F_{1,1797}$ = 35.69, p = 2.78 x 10^{-9}; see Figure 8B; Tables 4 and 5). This interaction was a result of dCA1→ACC PDC decreasing to a greater degree when the barrier was present compared to ACC→dCA1 PDC.

Table 4.
PDC B1 ANOVA Results by Rat, Implant Type, and Effect

Rat	Implant	Directionality	Barrier Presence	DxBP Interaction
A	ACC-VTA	$F_{1,1194}$ =362.56, p=5.57x10^{-72}	$F_{1,1194}$ =33.91, p=7.71x10^{-9}	$F_{1,1194}$ =46.82, p=1.16x10^{-11}
B	ACC-VTA	$F_{1,1194}$ =719.45, p=2.01x10^{-124}	$F_{1,1194}$ =121.57, p=5.46x10^{-27}	$F_{1,1194}$ =151.02, p=9.03x10^{-33}
C	ACC-VTA	$F_{1,1194}$ =351.65, p=4.24x10^{-74}	$F_{1,1194}$ =23.56, p=6.78x10^{-34}	$F_{1,1194}$ =54.22 p=3.96x10^{-29}
D	ACC-VTA	$F_{1,1194}$ =402.95, p=5.32x10^{-75}	$F_{1,1194}$ =14.08, p=2.00x10^{-4}	$F_{1,1194}$ =341.11, p=1.00x10^{-4}
E	ACC-VTA	$F_{1,1194}$ =352.77, p=2.78x10^{-68}	$F_{1,1194}$ =20.55, p=3.42x10^{-7}	$F_{1,1194}$ =88.45, p=4.64x10^{-22}
F	ACC-dCA1	$F_{1,1194}$ =242.50, p=1.44x10^{-50}	$F_{1,1194}$ =310.47, p=6.67x10^{-63}	$F_{1,1194}$ =30.40, p=5.02x10^{-8}
G	ACC-dCA1	$F_{1,1194}$ =528.33, p=2.15x10^{-99}	$F_{1,1194}$ =273.99, p=2.53x10^{-56}	$F_{1,1194}$ =70.1, p=1.36x10^{-16}

Table 4. Individual rat PDC ANOVA main and interaction effects by implant type in condition B1.

A

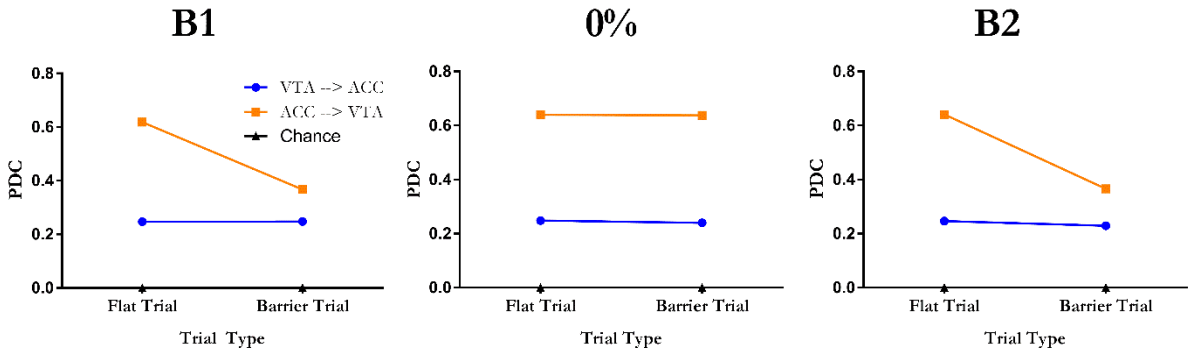

B

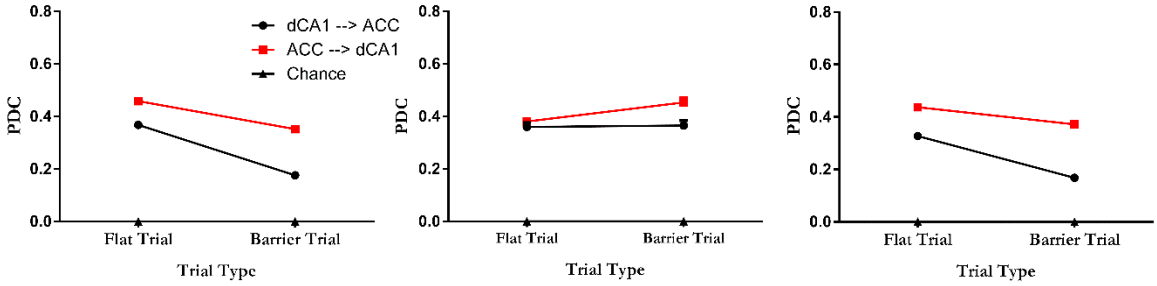

Figure 8. ACC causes ACC-VTA and ACC-dCA1 theta coherence as determined by partial directed coherence (PDC). **A.** ACC → VTA and VTA → ACC theta coherence on barrier trials across the three phases. **B.** ACC→ dCA1 and dCA1 → ACC theta coherence on barrier trials across the three phases. A are data from rat B; B are from rat G.

Table 5.
PDC B2 ANOVA Results by Rat, Implant Type, and Effect

Rat	Implant	Directionality	Barrier Presence	DxBP Interaction
A	ACC-VTA	$F_{1,596}$ =118.17, p=1.10x10^{-10}	$F_{1,596}$ =12.88, p=4.00x10^{-4}	$F_{1,596}$ =12.47, p=4.00x10^{-4}
B	ACC-VTA	$F_{1,596}$ =628.74, p=2.78x10^{-95}	$F_{1,596}$ =129.12, p=3.21x10^{-27}	$F_{1,596}$ =175.93, p=2.28x10^{-35}
C	ACC-VTA	$F_{1,596}$ =482.87, p=7.69x10^{-79}	$F_{1,596}$ =125.47, p=1.46x10^{-26}	$F_{1,596}$ =92.69, p=1.74x10^{-20}
D	ACC-VTA	$F_{1,596}$ =492.48, p=1.00x10^{-82}	$F_{1,596}$ =12.69, p=4.00x10^{-4}	$F_{1,596}$ =122.42, p=1.37x10^{-25}
E	ACC-VTA	$F_{1,596}$ =416.22, p=6.88x10^{-70}	$F_{1,596}$ =50.60, p=7.80x10^{-15}	$F_{1,596}$ =8.95, p=2.90x10^{-3}
F	ACC-dCA1	$F_{1,596}$ =197.36, p=7.36x10^{-39}	$F_{1,596}$ =100.61, p=5.66x10^{-22}	$F_{1,596}$ =17.18, p=3.89x10^{-5}
G	ACC-dCA1	$F_{1,596}$ =245.74, p=1.26x10^{-46}	$F_{1,596}$ =233.99, p=8.45x10^{-45}	$F_{1,596}$ =88.32, p=1.18x10^{-19}

Table 5. Individual rat PDC ANOVA main and interaction effects by implant type in condition B2.

Discussion

We investigated the influence of physical effort on VTA, ACC, and dCA1 theta (4-12 Hz) power, coherence, partial directed coherence (PDC), and running speed as rats ran a rectangular track requiring varying levels of effort to reach a fixed reward. PDC analysis of task-related casual relationships between brain areas revealed significant ACC → VTA and ACC → dCA1 directionality, the magnitude of which was modulated by the presence or absence of the barrier. Additionally, we found that ACC and VTA, but not dCA1, theta power, ACC-VTA coherence, running speed, and, surprisingly, ACC-dCA1 coherence increased as the rat entered the barrier-containing region of the maze on trials when the barrier was absent. In contrast, theta signals did not increase to the same degree across the same region of space when the barrier was present. In the reward region, however, ACC and VTA theta power and coherence as well as ACC-dCA1 theta coherence were independent of the effort condition.

These PDC results are consistent with prior reports showing cortical influence over VTA and dCA1. For example, Beier et al. (2015) found that the VTA dopaminergic neurons projecting to NAcc are directly regulated by anterior-cortical-VTA glutamatergic afferents and that rodents will self-stimulate those projections. Additionally, ACC control over the VTA is strongly implicated in inhibition of cocaine seeking (Navailles, Guillem, Vouillac-Mendoza, & Ahmed, 2015). Moreover, Rajasethupathy et al. (2015) found that ACC projections to dCA1 mediate memory retrieval and Ito et al. (2015) implicated ACC influence over dCA1 in directing goal-oriented place-cell activity. One interpretation of these findings is that ACC top-down projections to the VTA and dCA1 (Ferenczi et al., 2016; Fujisawa & Buzsaki, 2011; Taber et al., 1995) underlie a circuit via which cortical representations can update spatial and motivational brain states, enabling the translation of a cortical signal into a motivational drive which can modify behaviour.

Rats' running speeds significantly increased in the barrier region when the barrier was absent. This may have been due to the reduced physical demands of the task or, alternatively, may have been driven by increased motivation signals, perhaps provided in a top-down manner from the ACC. In either case, one consequence of this relationship is that changes in running speed are potentially confounded with some of the electrophysiological effects that we observed. Our analyses indicate, however, that the changes in electrophysiology we observed are over and above that which would be predicted from the changes in running speed *per se*. First, correlations between instantaneous power and instantaneous running speed for all times in all regions in all sessions while rats were moving (speed > 1 cm/s), were minimal and non-significant, suggesting that speed and

power were independently driven by the effort condition. Second, and most importantly, after statistically controlling for speed as a covariate in a multivariate regression model predicting theta power in the barrier region, the effort condition remained a highly significant factor in ACC and VTA (but not dCA1). Third, if the theta power changes were movement artefacts, it is difficult to explain why activity in the barrier region during the barrier condition, where rats would vigorously leap atop the barrier, was generally equal to that recorded in the initial stem of the apparatus where there was never a barrier.

Our results likely reflect the operation of several different mechanisms, with the possibility that more than one operates simultaneously. Two possible mechanisms include prediction error (Pearce & Hall, 1980) and negative reinforcement (Skinner, 1938). Prediction error theory posits that, based on prior experience and outcomes, the brain predicts what will happen in a similar situation and elicits a strong signal when an outcome violates that prediction. In our study, theta power in the ACC and VTA increased markedly when the barrier was absent. Framed as a prediction error effect, this would suggest that the baseline prediction might have been the presence of the barrier, such that the absence of the barrier was 'unexpected'. Prediction error, however, cannot fully account for our findings for several reasons: i) because rats were visually cued in the start box, despite a lack of evidence that they attended to the cues, we cannot rule out the possibility that they did register the cues and thus had accurate predictive information about the upcoming trial; ii) the elevated power and coherence responses occurred only when the barrier was absent, corresponding to the notion of a positively signed prediction error (Eshel et al., 2015; Kennerly et al., 2011), but inconsistent with other reports of unsigned, 'surprise', prediction errors (Bryden et al., 2011; Hayden, Heilbronner, Pearson, & Platt, 2011). Furthermore, were these signals true prediction error signals, the presence or absence of the barrier in the B1 condition, when the barrier was present on 50% of trials, should be equally surprising with each trial type eliciting a transient response.

Negative reinforcement (NR) models suggest that the removal of an aversive stimulus, such as a barrier, is itself a reinforcer (Skinner, 1938). Typical NR studies require subjects to emit an instrumental response to remove or avoid an aversive stimulus (Qi et al., 2016) and adapt future behaviour (Oleson, Gentry, Chioma, & Cheer, 2012). Although our study is slightly different from a typical NR design in that the omission of the barrier did not require an instrumental response, the increase in theta power and coherence along with running speed is consistent with the core notion of NR: the absence of a barrier, when it could have been present, is reinforcing. Taking into account the differences in our task design from typical NR studies, most importantly, the lack of an instrumental response to

omit the barrier, it is tempting to describe our findings as a neural correlate of 'relief': the chance avoidance of an aversive outcome (Carver, 2009; Sweeny & Vohs, 2012).

Our data integrates and extends the evidence indicating a close link between cortical states and activity in dopaminergic brain areas (Beier et al., 2015; Fujisawa & Buzsaki, 2011; Taber et al., 1995; Wu et al., 2013) and complements demonstrations of cortical control of other affective states, such as fear (Karalis et al., 2016; Likhtik, Stujenske, Topiwala, Harris, & Gordon, 2014) and apathy (Moretti & Signori, 2016; Onoda & Yamaguchi, 2015). Although prior studies have suggested roles for the ACC in commitment to a course of action (Hayden, Pearson, & Platt, 2011; Ma et al., 2014), encoding value associated with physical effort (Cowen, Davis, & Nitz, 2012; Friedman et al., 2015; Hillman & Bilkey, 2010; Parvizi, Rangarajan, Shirer, Desai, & Greicius, 2013; Rudebeck, Walton, Smyth, Bannerman, & Rushworth, 2009), and implicated ACC dysfunction as a risk factor for severe apathy (Njomboro et al., 2012), no prior reports have examined the route by which changes in cortical value states are translated into a motivational signal. The idea of a continuously sampling cortical value state complements reports of a similarly adaptive mesolimbic dopamine signal (Hamid et al., 2016; Howe et al., 2013) and provides an indication of at least some of the pathways via which this latter response could be modulated. Together, these data suggest that cortical and dopaminergic states modulate the motivation to pursue a reward, enabling organisms to behave flexibly in order to optimize available opportunities in uncertain, changing environments (Hayden, Pearson, & Platt, 2011). Future work will expand the mechanistic insight of this phenomenon by directly linking changes in the ACC to VTA projection with predicted changes in behavioral outcomes.

References

Baccalá, L., & Sameshima, K. (2001). Partial directed coherence: a new concept in neural structure determination. *Biological Cybernetics*, *84*(6), 463–474.

Beier, K. T., Steinberg, E. E., DeLoach, K. E., Xie, S., Miyamichi, K., Schwarz, L., … Liqun, L. (2015). Circuit architecture of VTA dopamine neurons revealed by systematic input-output mapping. *Cell*, *162*, 622–634.

Boykin, E. R., Khargonekar, P. P., Carney, P. R., Ogle, W. O., & Talathi, S. S. (2012). Detecting effective connectivity in networks of coupled neuronal oscillators. *Journal of Computational Neuroscience*, *32*(3), tr521-538.

Bryden, D. W., Johnson, E. E., Tobias, S. C., Kashtelyan, V., & Roesch, M. (2011). Attention for learning signals in the anterior cingulate cortex. *The Journal of Neuroscience*, *31*(50), 18266–18274.

Carver, C. S. (2009). Threat Sensitivity, Incentive Sensitivity, and the Experience of Relief. *Journal of Personality*, *77*(1), 125–138. https://doi.org/10.1111/j.1467-6494.2008.00540.x

Cavanagh, J. F., Frank, M. J., Klein, T. J., & Allen, J. J. B. (2010). Frontal Theta Links Prediction Errors to Behavioral Adaptation in Reinforcement Learning. *Neuroimage*, *49*(4). https://doi.org/10.1016/j.neuroimage.2009.11.080

Darwin, C. (1865). *On the orgin of species by means of natural selection, or the preservation of favoured races in the struggle for life*. New York: D. Appleton and Company. Retrieved from http://darwin-online.org.uk/converted/pdf/1861_OriginNY_F382.pdf

Eshel, N., Bukwich, M., Rao, V., Hemmelder, V., Tian, J., & Uchida, N. (2015). Arithmetic and local circuitry underlying dopamine prediction errors. *Nature*, *525*, 243–246.

Eshel, Tian, J., Bukwich, M., & Uchida, N. (2016). Dopamine neurons share common response function for reward prediction error. *Nature Neuroscience*, *19*(3).

Faget, L., Osakada, F., Duan, J., Ressler, R., Johnson, A. B., Proudfoot, J. A., … Hnasko, T. S. (2016). Afferent Inputs to Neurotransmitter-Defined Cell Types in the Ventral Tegmental Area. *Cell Reports*, *15*(12), 2796–2808. https://doi.org/10.1016/j.celrep.2016.05.057

Ferenczi, E., Zalocusky, K., Liston, C., Grosenick, L., Warden, M., Amatya, D., … Deisseroth, K. (2016). Prefrontal cortical regulation of brainwide circuit dynamics and reward-related behavior. *Science*, *351*(6268), aac9698-1-aac9698-12.

Fujisawa, S., & Buzsaki, G. (2011). A 4Hz oscillation adaptively synchronizes prefrontal, VTA, and hippocampal activities. *Neuron*, *72*, 153–165.

Gao Liu, C-L., Yang, S., Jin, G-Z., Bunney, B. S., Shi, W-X., M. (2007). Functional coupling between prefrontal cortex and dopamine neurons in the ventral tegmental area. *The Journal of Neuroscience*, *27*(20), 2414–5421.

Hamid, A., Pettibone, J., Mabrouk, O., Hetrick, V., Schmidt, R., Vander Weele, C., … Berke, J. D. (2016). Mesolimbic dopamine signals the value of work. *Nature Neuroscience*, *19*, 117–126.

Hayden, B., Pearson, J., & Platt, M. (2011). Neuronal basis of sequential foraging decisions in a patchy environment. *Nature Neuroscience*, *14*(7), 933–939.

Hayden, B. Y., Heilbronner, S. R., Pearson, J. M., & Platt, M. L. (2011). Surprise signals in anterior cingulate cortex: neuronal encoding of unsigned reward prediction errors driving adjustment in behavior. *The Journal of Neuroscience : The Official Journal of the Society for Neuroscience*, *31*(11), 4178–87. https://doi.org/10.1523/JNEUROSCI.4652-10.2011

Howe, M., Tierney, P., Sandberg, S., Phillips, P. E. M., & Graybiel, A. M. (2013). Prolonged dopamine signalling in striatrum signals proximity and value of distant rewards. *Nature*, *500*, 575–579.

Ito, H. T., Zhang, S.-J., Witter, M. P., Moser, E. I., & Moser, M.-B. (2015). A prefrontal-thalamo-hippocampal circuit for goal-directed spatial navigation. *Nature*, *522*, 50–55.

Karalis, N., Dejean, C., Chaudun, F., Khoder, S., Rozeske, R. R., Wurtz, H., … Herry, C. (2016). 4-Hz oscillations synchronize prefrontal–amygdala circuits during fear behavior. *Nature Neuroscience*, *19*(4), 605–612. https://doi.org/10.1038/nn.4251

Kennerly, S. W., Behrens, T. E. J., & Wallis, J. D. (2011). Double dissociation of value computations in orbitofrontal and anterior cingulate neurons. *Nature Neuroscience*, *14*(12), 1581–1589.

Likhtik, E., Stujenske, J. M., Topiwala, M. A., Harris, A. Z., & Gordon, J. A. (2014). Prefrontal entrainment of amygdala activity signals safety in learned fear and innate anxiety. *Nature Neuroscience*, *17*, 106–113.

Morales, M., & Margolis, E. B. (2017). Ventral tegmental area: cellular heterogeneity, connectivity and behaviour. *Nature Reviews Neuroscience*, *18*, 73–85. https://doi.org/10.1038/nrn.2016.165

Moretti, R., & Signori, R. (2016). Neural Correlates for Apathy: Frontal-Prefrontal and Parietal Cortical- Subcortical Circuits. *Frontiers in Aging Neuroscience*, *8*, 289. https://doi.org/10.3389/fnagi.2016.00289

Navailles, S., Guillem, K., Vouillac-Mendoza, C., & Ahmed, S. H. (2015). Coordinated Recruitment of Cortical–Subcortical Circuits and Ascending Dopamine and Serotonin Neurons During Inhibitory Control of Cocaine Seeking in Rats. *Cerebral Cortex*, *25*(9), 3167–3181. https://doi.org/10.1093/cercor/bhu112

Njomboro, P., Deb, S., & Humphreys, G. W. (2012). Apathy and executive functions: insights from brain damage involving the anterior cingulate cortex. *Case Reports*, *2012*(sep20 1), bcr0220125934-bcr0220125934. https://doi.org/10.1136/bcr-02-2012-5934

Oleson, E. B., Gentry, R. N., Chioma, V. C., & Cheer, J. F. (2012). Subsecond Dopamine Release in the Nucleus Accumbens Predicts Conditioned Punishment and Its Successful Avoidance. *Journal of Neuroscience*, *32*(42), 14804–14808. https://doi.org/10.1523/JNEUROSCI.3087-12.2012

Onoda, K., & Yamaguchi, S. (2015). Dissociative contributions of the anterior cingulate cortex to apathy and depression: Topological evidence from resting-state functional MRI. *Neuropsychologia*, *77*, 10–18. https://doi.org/10.1016/j.neuropsychologia.2015.07.030

Paxinos, G., & Watson, C. (1997). *The rat brain in stereotaxic coordinates 4th edition*. New York: Academic Press.

Pearce, J. M., & Hall, G. (1980). A Model for Pavlovian Learning: Variations in the Effectiveness of Conditioned But Not of Unconditioned Stimuli. *Psychological Review*, *87*(6), 532–552.

Qi, J., Zhang, S., Wang, H.-L., Barker, J., Miranda-Barrientos, M., & Morales, M. (2016). VTA glutamatergic inputs to nucleus accumbens drive aversion to acting on GABAeric interneurons. *Nature Neuroscience*, *79*, 725–733.

Rajasethupathy, P., Sankara, S., Marshel, J. H., Kim, C. K., Ferenczi, E., Lee, S. L., … Deisseroth, K. (2015). Projections from neocortex mediate top-down control of memory retrieval. *Nature*, *526*(653–659).

Salamone, J. D., & Correa, M. (2012). The Mysterious Motivational Functions of Mesolimbic Dopamine. *Neuron*, *76*(3), 470–485. https://doi.org/10.1016/j.neuron.2012.10.021

Skinner, B. F. (1938). *The behavior of organisms: an experimental analysis*. New York: Appleton-Century-Crofts.

Sweeny, K., & Vohs, K. D. (2012). On Near Misses and Completed Tasks: The Nature of Relief. *Psychological Science*, *23*(5), 464–468. https://doi.org/10.1177/0956797611434590

Taber, M. T., Das, S., & Fibiger, H. C. (1995). Cortical regulation of subcortical dopamine release:

545 mediation via the ventral tegmental area. *Journal of Neurochemistry*, *65*(3), 1407–1410.

546 Wu, J., Gao, M., Shen, J. X., Shi, W. X., Oster, A. M., & Gutkin, B. S. (2013). Cortical control of VTA
547 function and influence on nicotine reward. *Biochem Pharmacol*, *86*(8), 1173–1180.
548 https://doi.org/10.1016/j.bcp.2013.07.013

549